

THE KEY ROLE OF DYNAMICS IN THE CHROMOSPHERIC HANLE POLARIZATION

E.S. CARLIN¹, BIANDA M.¹

ABSTRACT

The quantum theory of polarized light allows to model scattering in the solar atmosphere for inferring its properties. This powerful approach has revealed two key long-standing problems in solar physics: the puzzling dilemmas between theory and observations in several anomalously polarized spectral lines; and the need of inferring the ubiquitous weak chromospheric magnetic fields, which requires discriminating the Hanle effect in dynamic optically thick plasmas. However, the ever-present dynamics, i.e. the temporal evolution of heatings and macroscopic motions, has been widely disregarded when modeling and interpreting the scattering polarization. This has hindered a consistent theoretical solution to the puzzle while falsifying the Hanle diagnosis. Here, we show that the dynamical evolution is a keystone for solving both problems because its systematic impact allows to explain the observations from “anomalous” instantaneous polarization signals. Evolution accounted for, we reproduce amplitudes and (spectral and spatial) shapes of the Ca I 4227 Å polarization at solar disk center, identifying a restrictive arrangement of magnetic fields, kinematics, heatings, and spatio-temporal resolution. We find that the joint action of dynamics, Hanle effect, and low temporal resolutions mimics Zeeman linear polarization profiles, the true weak-field Zeeman signals being negligible. Our results allow to reinterpret many polarization signals of the solar spectra and support time-dependent scattering polarization as a powerful tool for deciphering the spatio-temporal distribution of chromospheric heatings and fields. This approach may be a key aid in developing Hanle diagnosis for the solar atmosphere.

Subject headings: Polarization — scattering — radiative transfer — shock waves — Sun: chromosphere — stars: atmospheres

1. INTRODUCTION

Solar dynamics usually affects the emergent spectral line polarization in a complex way that cannot be explained as a mere Doppler effect. On one hand, velocity gradients produce variable opacity-changing Doppler shifts along the optical path of each ray. This affects the NLTE² atomic level populations and also changes and fragments the formation region of the spectral line in the atmosphere. Therefore, each wavelength of a polarization profile can be sensitive to one or more regions in height and hence to different conditions. On the other hand, there is the temporal evolution of the physical quantities, which shows rhythms of variation increasing with height while coexisting with low temporal resolution in the observations. Thus, spectropolarimetric recordings of the solar chromosphere are unresolved in time. This implies a coherent integration of the spectral profiles in the detector and therefore signal cancelations and changes of shape in the measured polarization. In addition, and regarding the linear polarization (LP) in Stokes Q and U (where the Hanle effect appears), there is also the lesser-known dynamic effect of *Doppler-induced polarization modulation* (e.g., Carlin et al. 2012). This is one of several effects linking the macroscopic state of the atmosphere with the atomic density matrix that describes the population imbalances and coherences between atomic energy sub-levels in each plasma element (atomic polarization; Landi Degl’Innocenti & Landolfi 2004, hereafter LL04). The key is that Doppler brightenings (Hyder & Lites 1970)

abruptly enhance the anisotropy of the radiation field in the presence of *organized gradients* of macroscopic motions (velocity) and/or of microscopic motions (temperature) in the stellar plasma, e.g. during a shock wave. In general, such dynamically induced anisotropic pumping modulates the atomic polarization and thus regulates the emission and absorption of LP.

Tornadoes (e.g., Wedemeyer-Böhm et al. 2012), quiet-Sun jets (Martínez Pillet et al. 2011), spicules (e.g., Hansteen et al. 2006), or supersonic flows (Borrero et al. 2010) proof the richness of dynamic processes in the sun. However, here we only shall refer to the most common motions affecting the bulk chromosphere: waves and convection.

Exposing the combined effects of dynamics in the scattering polarization requires detailed calculations in time-dependent models. Until now, this has only been done in Carlin et al. (2013) using unmagnetized models without spatial extension (e.g., Carlsson & Stein 1997). That paper (Fig. 8) shows how kinematics might dominate the evolution of spectral shapes, amplitudes, and signs in the scattering polarization. This problem avoids any true comparison between theory and observations of the thick solar atmosphere if the signals are not temporally resolved and dynamics, as is customary in our field, is neglected. Also, Hanle diagnosis becomes more difficult: magnetic and dynamic spectral signatures are indistinguishable. Thus, the lack of understanding of these points is a bottle neck for solar physics research, which needs proper measurements of magnetic fields above the photosphere.

In order to discriminate among polarization sources, the additional information encoded along dimensions

escarlin@irsol.ch

¹ Istituto Ricerche Solari Locarno, 6600 Locarno, Switzerland

² Non-local thermodynamical equilibrium.

where kinematic and magnetic effects behave different has to be considered. For instance, studying the spatial dimension, Carlin & Asensio Ramos (2015) revealed the existence of grooves with null polarization in synthetic maps of Ca II lines, and showed that such structures are a direct spatial fingerprint of the chromospheric magnetic field that are highlighted in presence of motions. The present work connects for the first time observations with MHD models through the synthesis of Hanle and Zeeman polarization in time, space, and wavelength.

2. CALCULATIONS

We considered time-dependent 3D R-MHD models of the solar chromosphere including non-equilibrium hydrogen ionization (Gudiksen et al. 2011; Carlsson et al. 2016) to solve the NLTE problem of the second kind (LL04, Chap. 14.1) for the CaI 4227 Å line at the disk center. The model was processed time step by time step (covering 15 minutes each 10 seconds) and column by column in both directions of a slit-like region ($\approx 0.''5 \times 33''$, see Fig.1), where the transfer of information among model columns was neglected (1.5D approximation).

First, we solved the NLTE ionization balance between CaI and CaII with the RH 1.5D code (Pereira & Uitenbroek 2015) considering partial redistribution (PRD) effects. We used a 20-level atomic model with 19 continuum transitions and 17 line transitions including the lower transitions of CaI and the ground level of CaII (Anusha et al. 2011). In a second step, the resulting atomic populations of the two levels of the 4226.72 Å CaI transition at each position and time were used to solve the polarized NLTE radiative transfer problem in the MHD model. Thus, we obtained the Stokes vector formed by atomic polarization, Hanle effect, and Zeeman effect in the regime of complete redistribution (LL04, Chap. 7). Here, we solved the statistical equilibrium equations, which determine the atomic density matrix including inelastic and depolarizing collisions in the impact approximation; and the radiative transfer equation for polarized light without stimulated emission in presence of an instantaneously stationary radiation field. Both the pure Zeeman signals in Q, U and V and the Hanle signals in Q and U (affected by atomic polarization and

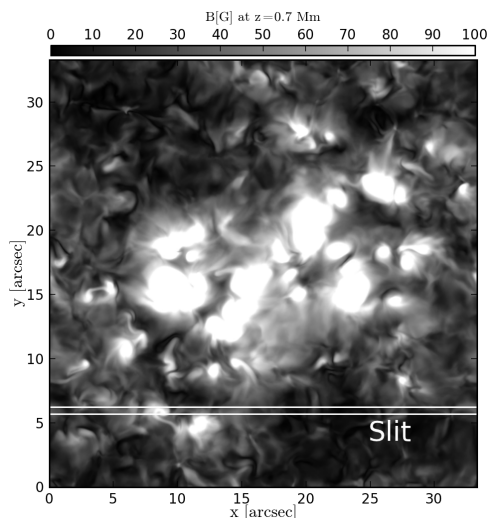


Figure 1. Magnetic intensity saturated in 100 G at $z=0.7$ Mm.

quantum coherences) were calculated such that the two contributions to the LP can be compared. Continuum polarization and PRD effects are negligible in the line core profiles emerging at disk center, namely for lines of sight in $\mu \approx [0.89, 1]$ (e.g., Dumont et al. 1977).

Finally, the synthetic Stokes vector components were integrated in time and space to emulate observations done by Bianda et al. (2011) at Irsol with a slit spectrograph and a ZIMPOL camera (Ramelli et al. 2010). We did all the calculations with microturbulent velocity $v_{micro} = 0$ and $v_{micro} = 2 \text{ km s}^{-1}$. Thus, our results combine ingredients never studied together before; namely, Hanle and Zeeman physics, time-varying magnetic fields, chromospheric kinematics and the final loss of spatio-temporal resolution.

3. RESULTS

The upper panel of Fig. 2 shows the chaotic life of the scattering polarization in a given time step of the simulation. These LP signals have large amplitudes (of up to 2.5%) and fast variations all over the temporal serie. Having the observations as reference, most instantaneous profiles are “anomalous” (see Fig. 3 and its caption). They have simple but sometimes not obvious explanations. Not infrequently, they show very sharp and clean peaks with striking similarity to many signals of the second solar spectrum in elements like BaI, TiI, CuI or other CaI lines not shown here. The temporal serie contains profiles with relatively small temporal, spatial and spectral coherence, which produces signal cancelations and reinforcements that are particularly dependent on kinematics when integrating.

The middle panels of Fig. 2 emulate the spatio-temporal integration resulting from a pixel size of $1.4''$ (as in our observations) and exposure time of 5 minutes (six times shorter than in our observations). These homogeneous polarization signals emerge naturally from the instantaneous profiles as the spatio-temporal resolution of our calculations is gradually decreased. Remarkably, the synthesis (middle panels of Fig. 2) and the observation (lower panels) have almost identical LP amplitudes only when integrating sufficient time to obtain a significant morphological resemblance. This fact suggests that in certain cases the LP rings present in the observations could be, as in our results, Hanle signals driven by kinematics instead of only the expected Hanle core with Zeeman or PRD side peaks. The LP rings in our observations come from internetwork (IN) patches. Weak-field features similar to such oval LP rings can be seen in other chromospheric lines of the second solar spectrum (e.g. $\lambda 8498$), sometimes as incomplete rings. In our simulation, they appear and disappear in different locations and gradually collapse to weaker one-lobe centered profiles for integrations $\gtrsim 8$ minutes (see the right-most panel in Fig 4). In other slit locations without rings, the long integrations deliver stronger monolithic (squared-like) one-lobe polarization bands along the spatial direction, as those appearing frequently in many observations of the second solar spectrum.

To obtain profiles compatible with the observations, the following ingredients are key. First, predominantly horizontal magnetic fields are needed for producing Hanle signals of sufficient amplitude at disk center.

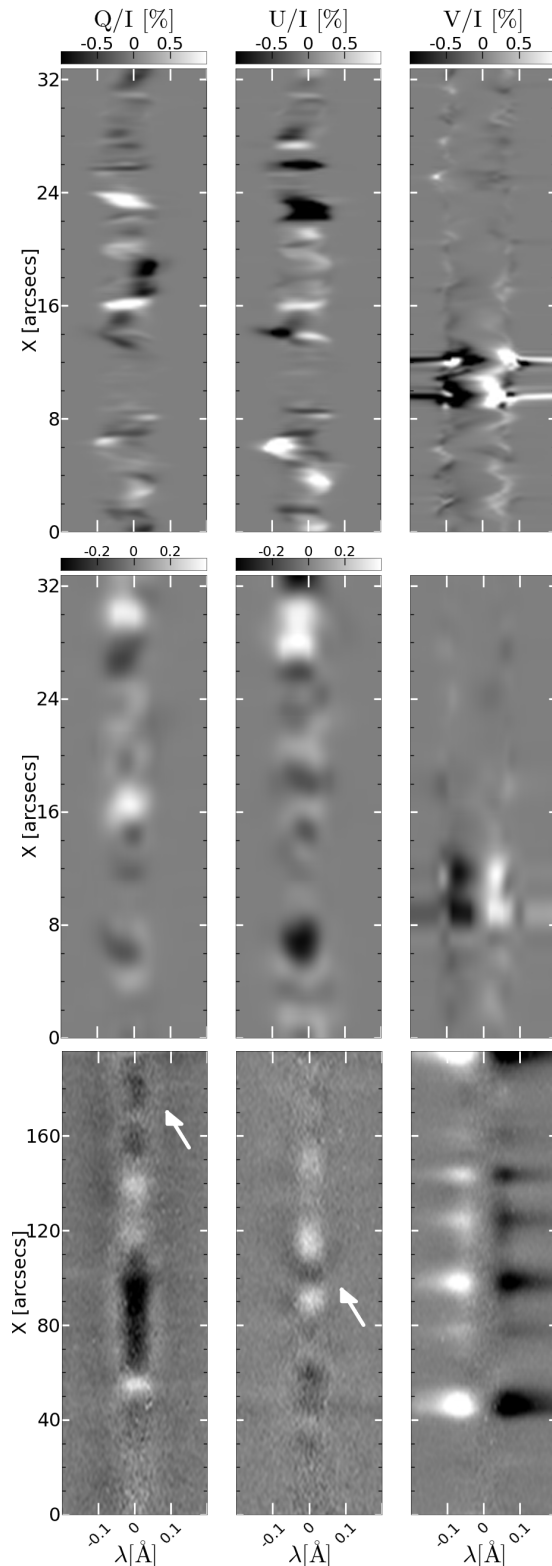


Figure 2. Polarization profiles of Ca I $\lambda 4227$ at disk center. Upper panels: synthetic slit observation for a spatio-temporal resolution of $0.''5$ (slit width) $\times 0.''2$ (along x) $\times 10$ s saturated to 1% in polarization (upper color bars). Middle panels: same as the upper panels but for a resolution of $0.''5 \times 1.''4 \times 5$ min. Lower panels: observation done with Zimpol@Locarno with a spectrograph slit of $0.''5$ wide and a resolution of $1.''4 \times 30$ minutes. LP in the middle and lower panels share the common color bars saturated to $\pm 0.4\%$.

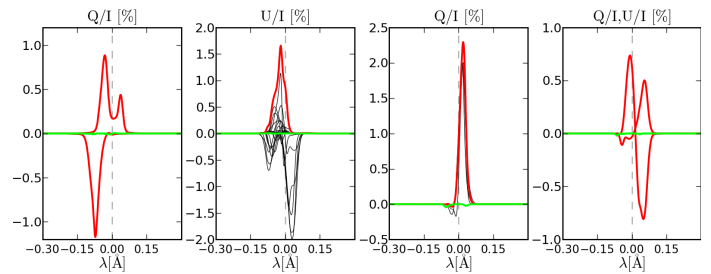


Figure 3. “Anomalous” Hanle signals in red. Corresponding Zeeman signal in green. Panel 1: triangular peaks. Panel 2: time evolution (black) around one timestep (red), leading to Zeeman-like signals. Panel 3: repetitive acute large signals in narrow wavelength intervals. Panel 4: very different Q and U shapes in same pixel, U very asymmetric, Q antisymmetric.

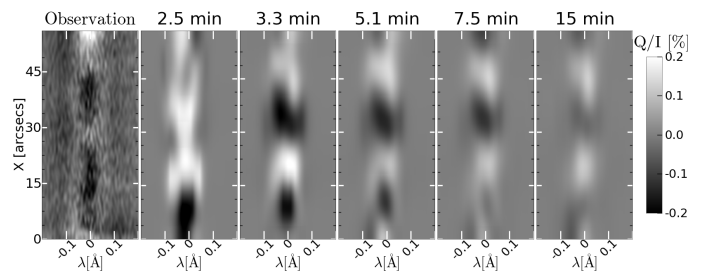


Figure 4. Left-most panel: $\lambda 4227$ LP rings in solar internetwork ($\Delta t \approx 30$ minutes). Remaining panels: evolution of synthetic polarization for the integration times Δt labeled. Color bar is common for all panels, but the spatial scale is only for observations: the synthetic scale is ≈ 4 times shorter.

Second, the amplification of the profiles produced by the Doppler-enhanced anisotropy in the presence of shock waves seems to be essential for having LP amplitudes as large as the observed ones after temporal integration. As the gradients of Doppler shifts along each ray change the angular distribution of the pumping field illuminating each scatterer, the atomic alignment of the levels of the transition also changes (Carlin et al. 2012). In the particular case of the $\lambda 4227$ spectral line, we find that the modulation of the upper level alignment (the only one that matters in this line) is strongly affected by the ever-present vertical gradients of velocity and temperature at the lower chromosphere. This is interesting because the line was expected to form in slightly lower layers without a large influence of velocities and because even considering the actual velocities they are not as strong as in the upper chromosphere. However, as the velocity *gradients* in relation to the Doppler broadening of the optical profiles are important, the subsequent amplifications of emergent LP also are. The net general effect of this situation in the emergent LP profiles is a dependence between their amplitude and the *absolute value* of the vertical velocity gradient among photosphere and chromosphere, similarly to what is explained in Carlin et al. (2013). This means that: (i) both emergent shock waves and gravity-driven plasma downflows tend to amplify the LP; and (ii) that the relative state of motion between chromosphere and photosphere matters because it regulates the Doppler brightening seen in the chromosphere.

A third ingredient notably affecting the signals is the

(roughly symmetric) Doppler oscillation of the emergent profiles around the line-center wavelength due to the periodic five-minute oscillation of the photosphere. This periodic motion acts as a large-scale offset velocity component for all the internetwork pixels of the slit, so shifting in frequency all slit profiles as a whole with time. Thus, if the thermal broadening is small, the spectral incoherence between different time steps notably alters the measured signals.

This connects with the fourth requirement: more heating at the low chromosphere. When all the calculations are done with zero microturbulent velocity, the integrated LP signals are too narrow and the even-narrower instantaneous LP profiles of the line occupy different halves of the core in opposite phases of the “supergranular” convection. Such a *lack of spectral coherence along time*, produced by these third and fourth ingredients, weakens the integrated LP signals. The resulting amplitudes are then too small everywhere ($< 0.1\%$ for an integration of 15 minutes), in comparison with observations. Note that as the observed LP signals are sizable in this line ($0.1 - 0.6\%$) after long integrations (typically $\gtrsim 15$ minutes), our synthetic profiles should also have similar amplitudes after integrating significantly. Thus, we find that a minimal ad hoc microturbulent velocity of 2 km s^{-1} (taken from semi-empirical models at temperature minimum) achieves this effect by synthesizing shapes and broadenings that partially reinforce the LP profiles along time³. Therefore, the spectral coherence of the signals in time can explain both large and negligible LP signals over relatively large areas. The need of extra broadening agrees with the fact that current MHD models do not fully reproduce the solar distribution of atmospheric heatings⁴. The last ingredient needed to mimic the observations is a minimum integration time of 5 minutes.

A reasonable combination of the same five physical ingredients can easily explain almost any known LP core of the second solar spectrum without resorting to physical arguments outside the standard theory of scattering polarization. The details depend on the particular atomic system (CaI 4227 Å here is just a reference line), the line of sight, and the solar evolution below the resolution element. Our delimitation of the dynamic effects is of interest because during many years a “solar origin” has been, somehow imprecisely, (dis)regarded by our community as an explanation to the enigmatic excesses of LP in several chromospheric line cores (e.g., Stenflo 2006). This is the first time that the relevance of such a solar component in the enigma is exposed and quantified.

Note that the coexistence of these ingredients in a quasi-periodic chromosphere gives integrated LP profiles mimicking transversal Zeeman signals (a central peak and side lobes of opposite sign), that compose the LP rings along the slit. The observed side LP lobes are typically associated with transversal Zeeman signals, but, surprisingly, such signals have negligible amplitudes (much lower than Hanle) everywhere in our simulations,

³ It also has a small effect in the atomic populations, hence in the polarization amplitudes.

⁴ As the solar atmospheric temperatures are larger than in current MHD models, microturbulence is needed to increase the broadenings. In our case, this means that the cool chromospheric plasma pockets where the spectral line forms should be hotter.

particularly after integration. Therefore, if the sun is well represented by these models, the transversal Zeeman effect can be neglected even close to areas with network-like magnetic strengths.

The spatial scale of our synthetic LP rings is small in comparison with observations (at least four times). They have apparent similar sizes in lower (solar) and middle (synthetic) panels of Fig. 2 only because the ratios between the loops length and the slit length are casually similar. Besides, exposure times larger than 5–8 minutes destroy all rings in our simulation, being these numbers also smaller (6–4 times) than in the observations available. Such differences do not affect our previous findings because the selected areas in the sun and in the models can naturally have different dynamical scales. However, they can help us to quantify the physical contributions to the LP rings and to test the MHD models.

LP rings can be seen as having two components: the central portion linking two rings, and the lateral envelope (the “sigma” components). Dynamic Hanle, Zeeman effect and remnant PRD effects (though observations were taken at $\mu = 0.94$) can contribute to explaining those components. The easiest explanation for the differences in the spatial scales is that the envelope of the rings is dominated by near-core PRD effects because is the only ingredient that we did not model and because it is (in principle) independent on the short dynamical scales of the chromosphere. If this is correct, our results points out that dynamics plays a significant role in the understanding of PRD effects close to disk center because the shifted LP peaks created by Hanle and amplified by dynamics lie above the near-core PRD wavelengths (yet, they form at different heights).

If the solar LP rings are entirely produced only by Hanle and dynamics, as in our calculations, the only explanation for the differences is in the scales of the model atmosphere. In this case, the LP rings are necessarily due to the overlap of horizontal fields (Hanle effect) and vertical kinematics; therefore, the scales of the LP rings must be guided by the *spatio-temporal coherence* of those factors. Our simulations and additional observational evidences (see the complementary paper) strongly support that this explains the linking point of the rings. However, for reproducing the long envelopes *just* with dynamic Hanle, the only possibility requires MHD models with a more periodic (repetitive) emergence of shock waves *everywhere*. Then, the mere temporal integration can create the illusion of symmetric LP rings (as in our simulations), even when the emergence of shocks is incoherent from pixel to pixel, simply because the reaction of the polarization to emergent waves is roughly the same everywhere in the IN. Our synthetic LP rings do not exist with temporal resolution.

The differences in scale, the particular entanglement of chromospheric heatings and motions in the LP amplitudes and the influence of time in the polarization indicate that our approach, based on temporal evolution of spatio-spectral patterns, may significantly help to understand/model the origin and distribution of heatings and motions in the quiet chromosphere.

We remark that the agreement in amplitudes and shapes between synthesis and observations of scattering polarization cannot be reproduced without the combination of *magneto-hydro-dynamics*, its action in the

atomic polarization (Hanle effect, enhanced anisotropy, and NLTE), time evolution, and spatio-temporal integration. This is a quiet restrictive situation. Avoiding only one ingredient, any agreement with observations disappears. Ignoring more than one, typically all of them except the Hanle effect and NLTE, one still can fit individual average profiles using free ad hoc parameters but the cost is a large degeneracy. Such a ‘static’ approach has been the standard in our field most of its history. Therefore, we point out the simple fact that the entanglement of several ingredients in different dimensions produce tight solutions. In this work, the smaller degeneracy is exposed as two-dimensional slit patterns, and the free parameters linking models with observations are a minimal well-constrained microturbulent velocity and a tunable integration time.

4. CONCLUSIONS

Our results show the second solar spectrum from a new perspective. Chromospheric scattering polarization should not be interpreted as instantaneous profiles, unaffected by time and macroscopic motions, hence disconnected from the essence of the chromosphere. Instead of symmetric static LP profiles, it seems that we actually observe the average of entangled dynamic effects that follow certain basic rules. Almost literally, solar dynamics sculpts the spectral line polarization through amplitude enhancements at particular Doppler shifts and their quasi-periodic repetition. The instrumental resolution and the spectral coherence of the enhancements make the rest. This situation affects all chromospheric signals of the second solar spectrum because the fundamental atomic sensitivity to anisotropic motions is intrinsic to scattering polarization and the measurements are temporally unresolved. However, low-chromosphere spectral lines should be particularly sensitive to dynamics. Our results point out that it is precarious to associate, as done in the literature, the existence of polarization anomalies with theoretical issues without first understanding how the atomic system reacts to dynamics in time and space. In that process, we have found natural explanations for such anomalies.

Our synthesis of the chromospheric $\lambda 4227$ scattering signals neglects the effect of horizontal inhomogeneities but includes vertical velocity gradients, collisions, magnetic fields, and time evolution. This leads to an unprecedented agreement with observations because it allows us to mimic entire spatial patterns along the slit considering the temporal integration. Furthermore, the agreement is adjusted only by quantities related with elements that are susceptible to improvement in the models (temperature and spatio-temporal scales). Any agreement seems impossible if the combined action of dynamics and Hanle effect in the atomic polarization is neglected: without dynamic effects, the signals are too faint to be detected. Thus, although the effects of the vertical velocity gradients in the LP were a priori difficult to identify in observations because several effects overlap, the constraints introduced in LP by the situation at disk center expose their existence.

The CaI 4227 Å line has been key. As the $\lambda 8498$ line, $\lambda 4227$ forms in cool low-chromosphere areas and hence is prone to be particularly sensitive to kinematic ampli-

fications of polarization. However, $\lambda 4227$ is intrinsically much stronger, so it can produce measurable LP amplitudes also at disk center, where it is possible to avoid confusing polarization sources (e.g., the solar limb) and constrain the analysis.

We also conclude that Hanle effect and dynamics can emulate transversal Zeeman signals and change the near-core PRD peaks in polarization. Caution is advised when interpreting observations without temporal resolution and when using Zeeman inversion codes where the Hanle signals are sizable.

Once the situation has been exposed in a spectral line of reference, the next step is to understand the behavior of other atomic systems in the presence of dynamics. In particular, the discrimination of effects producing the envelope of the LP rings and the role of dynamics in partial redistribution effects will be studied in additional publications.

This work was financed by the SERI project C12.0084 (COST action MP1104) and by the Swiss National Science Foundation project 200021_163405. Financial support given by the Aldo e Cele Daccò foundation is also gratefully acknowledged.

REFERENCES

- Anusha, L. S., Nagendra, K. N., Bianda, M., Stenflo, J. O., Holzreuter, R., Sampoorna, M., Frisch, H., Ramelli, R., & Smitha, H. N. 2011, *ApJ*, 737, 95
- Bianda, M., Ramelli, R., Anusha, L. S., Stenflo, J. O., Nagendra, K. N., Holzreuter, R., Sampoorna, M., Frisch, H., & Smitha, H. N. 2011, *A&A*, 530, L13
- Borrero, J. M., Martínez-Pillet, V., Schlichenmaier, R., Solanki, S. K., Bonet, J. A., del Toro Iniesta, J. C., Schmidt, W., Barthol, P., Gandorfer, A., Domingo, V., & Knölker, M. 2010, *ApJ*, 723, L144
- Carlin, E. S., & Asensio Ramos, A. 2015, *The Astrophysical Journal*, 801, 16
- Carlin, E. S., Asensio Ramos, A., & Trujillo Bueno, J. 2013, *ApJ*, 764, 40
- Carlin, E. S., Manso Sainz, R., Asensio Ramos, A., & Trujillo Bueno, J. 2012, *ApJ*, 751, 5
- Carlsson, M., Hansteen, V. H., Gudiksen, B. V., Leenaarts, J., & De Pontieu, B. 2016, *A&A*, 585, A4
- Carlsson, M., & Stein, R. F. 1997, *ApJ*, 481, 500
- Dumont, S., Pecker, J. C., Omont, A., & Rees, D. 1977, *A&A*, 54, 675
- Gudiksen, B. V., Carlsson, M., Hansteen, V. H., Hayek, W., Leenaarts, J., & Martínez-Sykora, J. 2011, *A&A*, 531, A154
- Hansteen, V. H., De Pontieu, B., Rouppe van der Voort, L., van Noort, M., & Carlsson, M. 2006, *ApJ*, 647, L73
- Hyder, C. L., & Lites, B. W. 1970, *Sol. Phys.*, 14, 147
- Landi Degl’Innocenti, E., & Landolfi, M. 2004, *Polarization in Spectral Lines* (Kluwer Academic Publishers)
- Martínez Pillet, V., Del Toro Iniesta, J. C., & Quintero Noda, C. 2011, *A&A*, 530, A111
- Pereira, T. M. D., & Uitenbroek, H. 2015, *A&A*, 574, A3
- Ramelli, R., Balemi, S., Bianda, M., Defilippis, I., Gamma, L., Hagenbuch, S., Rogantini, M., Steiner, P., & Stenflo, J. O. 2010, *SPIE*, 77351Y
- Stenflo, J. O. 2006, in *Astronomical Society of the Pacific Conference Series*, Vol. 358, *Astronomical Society of the Pacific Conference Series*, ed. R. Casini & B. W. Lites, 215
- Wedemeyer-Böhm, S., Scullion, E., Steiner, O., Rouppe van der Voort, L., de La Cruz Rodríguez, J., Fedun, V., & Erdélyi, R. 2012, *Nature*, 486, 505